RSC Advances

PAPER

View Article Online
View Journal | View Issue

Cite this: *RSC Adv.*, 2020, **10**, 44601

Antibacterial activity of AgNPs–TiO_2 nanotubes: influence of different nanoparticle stabilizers

Ondrej Bilek,[a] Tatiana Fialova,[b] Alexandr Otahal,[c] Vojtech Adam,[ab] Kristyna Smerkova[ab] and Zdenka Fohlerova[*acd]

Received 25th August 2020
Accepted 1st December 2020

DOI: 10.1039/d0ra07305a

rsc.li/rsc-advances

Enhanced antibacterial properties of nanomaterials such as TiO_2 nanotubes (TNTs) and silver nanoparticles (AgNPs) have attracted much attention in biomedicine and industry. The antibacterial properties of nanoparticles depend, among others, on the functionalization layer of the nanoparticles. However, the more complex information about the influence of different functionalization layers on antibacterial properties of nanoparticle decorated surfaces is still missing. Here we show the array of ~50 nm diameter TNTs decorated with ~50 nm AgNPs having different functionalization layers such as polyvinylpyrrolidone, branched polyethyleneimine, citrate, lipoic acid, and polyethylene glycol. To assess the antibacterial properties, the viability of Gram-positive (*Staphylococcus aureus*) and Gram-negative bacteria (*Escherichia coli* and *Pseudomonas aeruginosa*) has been assessed. Our results showed that the functional layer of nanoparticles plays an important role in antibacterial properties and the synergistic effect such nanoparticles and TiO_2 nanotubes have had different effects on adhesion and viability of G^- and G^+ bacteria. These findings could help researchers to optimally design any surfaces to be used as an antibacterial including the implantable titanium biomaterials.

Introduction

Antibacterial properties of metals,[1] metal oxides[2] and alloys[3] have found significant use in clinics and industry. The protection of medical and surgical devices, clothes, or implantable materials from the growth and colonization of bacteria becomes the key factor for avoiding the transmission of infectious diseases or the acceptance of foreign materials in the host body.[4] However, bacterial contamination, resistance to antibiotics, and the development of biofilms still pose hard-to-solve problems with many implants and medical devices.

The inhibition of bacterial adhesion and growth comes from the natural antibacterial properties of materials such as copper, titanium, zinc, silver, and their alloys.[5] Nevertheless, many materials must be extra-modified to introduce the antibacterial coating based on chemically attached antibacterial peptides,[6] metal oxides,[2] organosilanes[7] or polymers[8] in order to inhibit the bacteria adhesion, growth and plaque formation. Besides, bacteria can also be killed based on photocatalytic properties of specific materials that have been successfully applied in water purification or air cleaning.[9] The inorganic nanomaterials such as metal/metal oxide nanoparticles (NPs) and the nanostructured surface of metallic biomaterials have a great impact on their ability to be utilized for the bacterial growth inhibition and the prevention of biofilm formation that protects bacteria against antibiotics.[10] The NPs size and shape[11] and the topography of the nanostructured surface, including the type of the material can effectively modulate the antibacterial properties.[12] Nevertheless, the mechanism of action is still being under the investigation. Some proposed theories speak about dissolved metal ion toxicity or generation of reactive oxygen species on the nanomaterial surface.[13] Apart from these, the anti-adhesive surface may arise from the morphological and physico-chemical properties of materials.[14] Even if the antibacterial properties of specific nanoparticles synthesized from Ag, Ti, Au, Zn, and its oxides are well known against both Gram-positive (*Bacillus subtilis*, *Staphylococcus aureus*) and Gram-negative bacteria (*Escherichia coli*, *Pseudomonas aeruginosa*), the impact of nanostructured surfaces has got attention in the last decades.[15]

Ti and its alloys have been applied in biomedicine for many years.[16] The smooth surface of titanium implants does not appear to be sufficiently bioactive and suffer from infections and fibrous tissue development. Therefore, the TiO_2 nanotubes with nanoscaled topography become an interesting nanomaterial to be recognized as an attractive and promising for biomedicine.[17,18] TNTs have been found to have good corrosion resistance, biocompatibility, hemocompatibility, and enhanced

[a]*Central European Institute of Technology, Brno University of Technology, Purkynova 123, Brno, Czech Republic. E-mail: zdenka.fohlerova@ceitec.vutbr.cz*
[b]*Department of Chemistry and Biochemistry, Mendel University in Brno, Zemedelska 1, Brno, Czech Republic*
[c]*Department of Microelectronics, Brno University of Technology, Technicka 10, Brno, Czech Republic*
[d]*Department of Biochemistry, Faculty of Medicine, Masaryk University, Kamenice 753/5, 625 00 Brno, Czech Republic*

bioactivity.[19,20] Moreover, a nanostructured surface can modulate the protein adsorption and cellular responses such as adhesion, proliferation, or differentiation and antibacterial properties.[21] In a positive way, the enhanced or stimulated biological response due to the nanostructured TiO_2 surface may be considered to mimic the natural cellular environment.

The TNTs have been demonstrated to be a promising platform for a drug loading and delivery administration.[22] The simple and controllable fabrication of highly ordered TNTs *via* electrochemical anodization process has been found to perform tunable drug-release of vancomycin[23] or gentamicin.[24] In addition to antibiotics loading, the doping with strontium and samarium[25] or decoration with nanoparticles such as gold,[26,27] zinc oxide,[28] selenium,[29,30] and silver[31,32] have been demonstrated to enhance the antibacterial properties of TNTs.[33–38] The antimicrobial properties of nanoparticles depend on the surface charge, nanoparticle size, shape, and surface coating (stabilizers/functional layers). Lately, the role of nanoparticle surface coatings became more apparent.[39] To date, colloidal nanoparticles with different surface coatings have been synthesized and evaluated for their antibacterial action.[40,41] However, the antibacterial properties of a free and decorated nanoparticles are supposed to significantly differ. To our knowledge, there is no information about the synergistic antibacterial effect of TiO_2 nanotubes and Ag nanoparticles with different functional layers.

In our work, the array of ~50 nm diameter TiO_2 nanotubes has been fabricated *via* anodic oxidation of polished titanium foil. Subsequently, the nanotubes were decorated with commercial silver nanoparticles of ~50 nm diameter. Nanoparticles were functionalized by polyvinylpyrrolidone, branched polyethyleneimine, citrate, lipoic acid and polyethylene glycol. Ag-decorated TNT arrays were characterized by scanning electron microspopy, atomic force microscopy and X-ray photoelectron spectroscopy. To assess the antibacterial properties, the adhesion and viability of Gram-positive (*S. aureus*) and Gram-negative bacteria (*E. coli* and *P. aeruginosa*) were performed. Our results showed that the functionalization layers of nanoparticles play an important role in antibacterial properties and should be considered when designing antibacterial surfaces.

Materials and methods

Anodic oxidation of titanium foil

The 0.125 mm thick titanium foil sheets (GoodFellow, 99.6+%, annealed) were degreased in acetone and isopropyl alcohol and polished with fabric disks and diamond suspension. TiO_2 nanotubes were fabricated by single-step anodic oxidation in the electrolyte solution composed of ethylene glycol (Penta, CZ), 1.2 wt% ammonium fluoride (Sigma Aldrich) and 2 vol% of deionized water (Millipore Corp., USA, 18.2 MΩ).[42] Electrochemical anodization was performed with a voltage ramp between 0 V and 30 V with a ramp speed of 1 V s^{-1}. The anodization time was 30 minutes per sample. After the anodization, samples were rinsed with deionized water and dried with a nitrogen stream. The TNTs samples were subsequently annealed in a vacuum furnace at 450 °C for 3 hours.

Decoration of TNTs with Ag-NPs

The array of TiO_2 nanotubes was decorated with commercial silver nanoparticles functionalized with polyvinylpyrrolidone (PVP), citrate, branched polyethyleneimine (BPEI), polyethylene glycol (PEG), and lipoic acid (Sigma-Aldrich; 0.02 mg mL^{-1} stock solutions) as depicted in Fig. 1. Because different nanoparticles exhibited different degree of adsorption rates onto the TiO_2 nanotubes, we optimized the dilution of stock solution for each nanoparticle to achieve the same number of nanoparticles

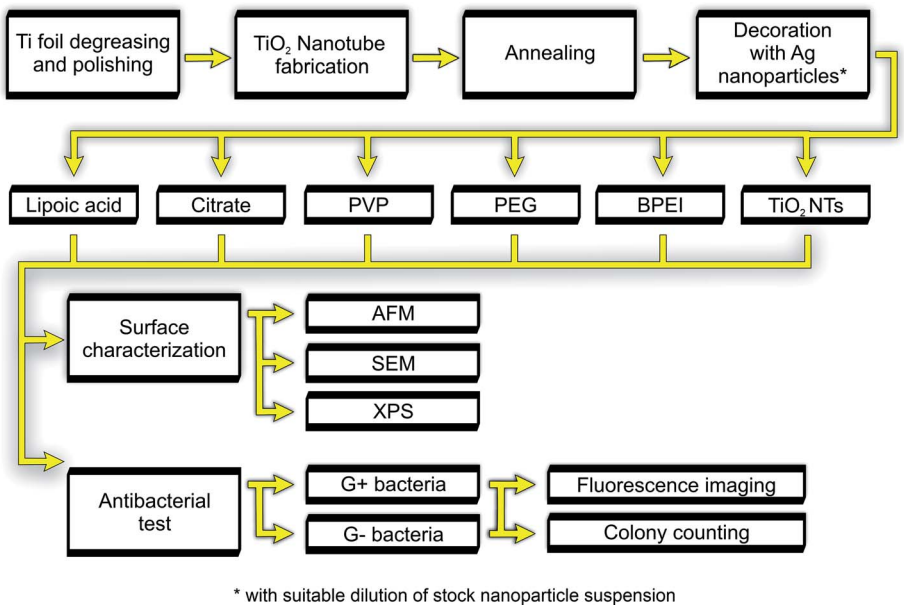

Fig. 1 General experimental flow chart.

per surface area. Then, 15 μL of diluted nanoparticle suspension was dropped onto the heated TNTs surface until drying. Decorated samples were rinsed five times in deionized water and soaked in ultrapure water to remove any un-adsorbed nanoparticles. The morphology of AgNPs-TNTs array was characterized with scanning electron microscope (SEM, Mira II, Tescan, CZ), surface roughness was analyzed using atomic force microscopy (AFM) in dry non-contact mode (SPM, Dimension Icon, Bruker), and X-ray photoelectron spectroscopy has been used to analyze surface chemistry (XPS, AXIS Supra, Kratos Analytical Ltd, UK). XPS spectra were analyzed by a peak fitting software (CasaXPS version2.3.18PR1.0) provided by SPECS GmbH (Berlin, Germany).

Bacterial cultures and SEM microscopy

Bacterial strains of *S. aureus* (CCM 4223), *E. coli* (CCM 3954), and *P. aeruginosa* (CCM 3955) were purchased from the Czech Collection of Microorganisms (CZ). After overnight cultivation at 37 °C on blood agar, the strains were diluted in Mueller Hinton broth (Oxoid, UK) to the concentration of 1×10^6 CFU mL^{-1} (where CFU is colony-forming unit), measured by optical density at 600 nm (OD600). To image the bacteria on the TNTs surface using the SEM microscopy, 2 mL of bacterial suspension was dropped on TNTs (control) and AgNPs-TNTs array and incubated at 37 °C for 5 hours. Then, the samples were three-times gently washed with sterile physiological solution. Bacteria were fixated in 2% glutaraldehyde for 1 hour. The dehydration step was performed using graded ethanol concentration of 30%, 50%, 70%, 80%, 90%, 95% and 100%, one time for each and twice in 100% for 15 min each. Dried samples were coated with a 10 nm thick gold layer in order to achieve a better contrast of bacteria.

Antibacterial test

Live/dead fluorescence staining was performed to image and count the live and dead bacteria on the TNTs and AgNPs-TNTs surface. Samples were rinsed with sterile ultrapure water and left to dry in sterile conditions. The dried samples were subsequently placed in sterile 12-well plate, bathed in 2 mL of bacterial inoculum and incubated for 24 hours at 37 °C. After the incubation, samples were washed five times with sterile saline. The staining of bacteria with Live/Dead BacLight Bacterial Viability and Counting Kit (Thermo Fisher Scientific) was performed as recommended by the manufacturer. The samples were observed by inverted fluorescence microscope Olympus IX71 (Olympus, Japan) at a magnification of 20×. Captured images were analyzed with ImageJ software. The contrast, brightness, and the displayed range (max, min) were adjusted with the brightness/contrast tool until individual bacteria became clearly visible. The area occupied by red (or green) color was selected using the color threshold and calculated using the measurement module. The value in pixels was divided by the total number of pixels present in the analyzed image, and the area of bacterial coverage (in percentage) specific for live and dead bacteria was calculated.

Antibacterial properties of silver NPs decorated nanotubes were further evaluated *via* colony counting method. A bacterial inoculum with a density of 10^8 CFU mL^{-1} was prepared as the stock solution. Samples were rinsed in sterile water and 100 μL of bacterial suspension was spread onto the surface, followed by 4 hours' incubation at 37 °C. Subsequently, the samples were gently rinsed in PBS and adhered bacteria were de-attached by vortexing and sonication. Collected bacterial suspension was diluted 100 times with PBS. The 200 μL of diluted solution was inoculated on agar plates and incubated for 24 hours at 37 °C and 80% humidity. Bacteria colonies were then counted and colony forming unit was calculated (CFU mL^{-1}).

Statistical analysis

Mean values and standard deviations of obtained data were calculated. Statistically significant differences ($p < 0.05$) were confirmed using Student's *t*-test. All shown data are expressed as the mean ± standard deviation. Coverage values are calculated from 5 images with the area of 558.7 × 419 μm per each sample and bacterium. Colony counting method was performed in duplicate.

Results and discussion

Characterization of TNTs and AgNPs–TNTs surface

TiO_2 nanotubes decorated with silver nanoparticles were fabricated *via* single-step anodic oxidation of titanium foil, followed by adsorption of commercially available silver nanoparticles of similar diameter but having a different functionalization layer (PVP, BPEI, citrate, PEG and lipoic acid). TNTs array without nanoparticles was taken as a control. SEM image analysis of nanostructured surface resulted in highly ordered TNTs with a diameter of 51.11 ± 5.77 nm as depicted in Fig. 2.

The surface roughness of the undecorated TiO_2 nanotubes was characterized using AFM. Fig. 3A shows the 3D morphology of TNTs. The surface roughness measured by AFM was approximately 24.34 nm. In order to confirm the uniform distribution of Ag nanoparticles on the TNTs surface, several

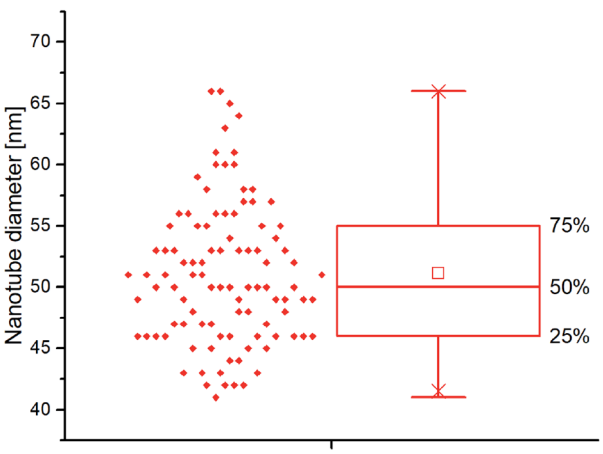

Fig. 2 Boxplot of nanotube diameter distributions calculated from SEM images.

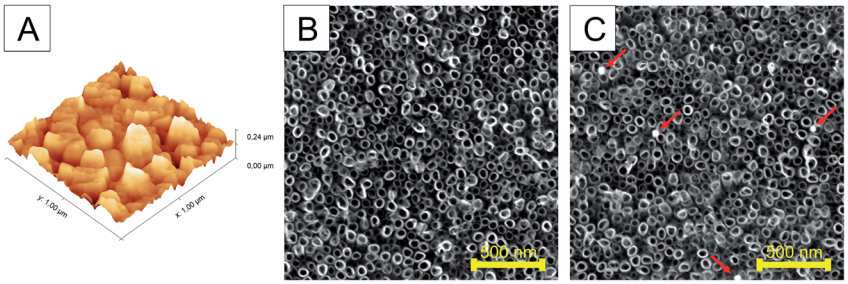

Fig. 3 AFM image showing root-mean-square (RMS) surface roughness of TNTs (A) and SEM image of as-annealed non-decorated TiO_2 nanotubes prepared by single-step anodic oxidation (B) and silver-decorated TiO_2 nanotubes (C). The nanoparticles are indicated by arrows.

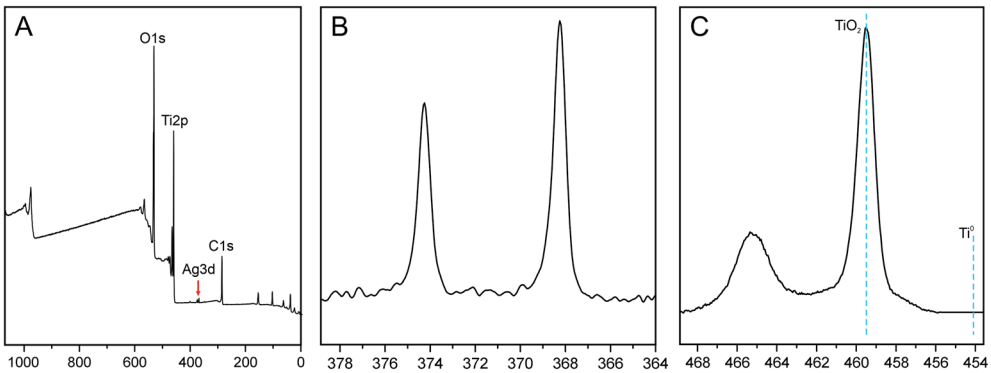

Fig. 4 XPS survey of TiO_2 nanotubes decorated with AgNPs (A), high resolution Ag 3d spectra (B) and high resolution spectra Ti 2p (C).

independent SEM images were evaluated for the number of nanoparticles per scanned area. The analysis of SEM images confirmed the decoration of TNTs surface with 3–4 nanoparticles on the area of 4 μm^2 for each of differently functionalized Ag nanoparticles (Fig. 3B and C). The size of nanoparticles of ~50 nm also guaranteed their deposition on the top of nanotubes.

The presence of silver nanoparticles and chemical composition of TiO_2 surface for bare- and silver-modified samples was investigated by X-ray photoelectron spectroscopy (XPS). In Fig. 4A, a typical XPS survey of the TiO_2 surface after AgNPs decoration is shown. The survey shows the Ti, C, O and Ag signals, indicating that silver nanoparticles are adsorbed on the TiO_2 nanotubes. Four main elements, *i.e.* Ti 2p, O 1s, C 1s and Ag 3d were quantitatively analyzed in details and XPS data is summarized in Table 1. Data shows that samples did not differ significantly in their compositions and chemical state of elements. All the samples possessed high carbon level on the surface in the range of 31–33%, which could be attributed to used electrolyte, or/and adsorbed CO_2 from the air. The silver content ~0.2% was indicated for all AgNPs decorated samples and no silver peak was observed for bare nanotubes. Similar Ag values on all samples also indicate that nanotubes were coated with nanoparticles evenly.

The characteristic high resolution XPS spectra of the Ag 3d region is shown in Fig. 4B. The signals at binding energies of 368 eV and 374 eV were corresponding to the $3d_{5/2}$ and $3d_{3/2}$ orbits of Ag^0 (metallic silver). The nanoparticles are not oxidized, as no further peaks at lower BE energy were needed for the fit. Additionally, high resolution XPS spectra of the Ti 2p is shown in Fig. 4C. The Ti $2p_{3/2}$ peak has a maximum at 459 eV which can be assigned to TiO_2. There is no contribution from metallic Ti (BE = 453.8 eV) which could be attributed to a thickness of oxide layer (> 10 nm).

Antibacterial properties of AgNPs-TNTs surfaces

The array of TiO_2 nanotubes has been previously found to exhibit antibacterial action in a certain extent compared to the flat surface but it still has been clearly insufficient for use as an antibacterial surface. On the other hand, the silver nanoparticles exhibited strong antimicrobial performance against wide spectra of microorganisms.[43] Although the mechanism of their antimicrobial action is not clearly understood, several mechanisms have been proposed. Those include the continual

Table 1 XPS analysis of bare-(control) and AgNPs decorated TiO_2 nanotubes. Relative percentage of selected elements calculated from narrow spectra

	BPEI [%]	Citrate [%]	Lipoic [%]	PEG [%]	PVP [%]	Control [%]
O 1s	51.42	50.28	50.74	51.49	51.29	51.07
Ti 2p	16.95	16.02	15.66	16.75	15.98	16.42
C 1s	31.44	33.5	33.41	31.56	32.52	32.51
Ag 3d	0.19	0.19	0.19	0.2	0.21	0

release of silver ions, disruption of the bacterial envelope, deactivation of respiratory enzymes, and generation of intracellular reactive oxygen species; consequently, cell death occurs.[44,45] The antimicrobial activity of nano-sized silver particles was also found size- and shape-dependent, one of the reasons could be that different morphologies provide different areas to interact with bacteria and thus results in different antibacterial efficiency. In accordance with most reported data, the smallest-sized spherical AgNPs (<50 nm) were more efficient to kill G^- bacteria as compared to larger spherical AgNPs. Moreover, nanoparticles are usually stabilized in solution with a wide spectrum of chemicals such as citrate, polyvinylpyrrolidone *etc.* A few stabilization agents and/or functional layers of nanoparticles have been previously reported to affect the cell–surface interaction resulting in different antibacterial action.[39,46] Since the nanoparticle stabilizers have not been extensively investigated for their antibacterial action of adsorbed nanoparticles, here we compared five different NPs stabilizing agents by the decoration of AgNPs on TNTs nanotubes. The synergistic antibacterial activity was evaluated for three bacteria such as *E. coli*, *P. aeruginosa* and *S. aureus*.

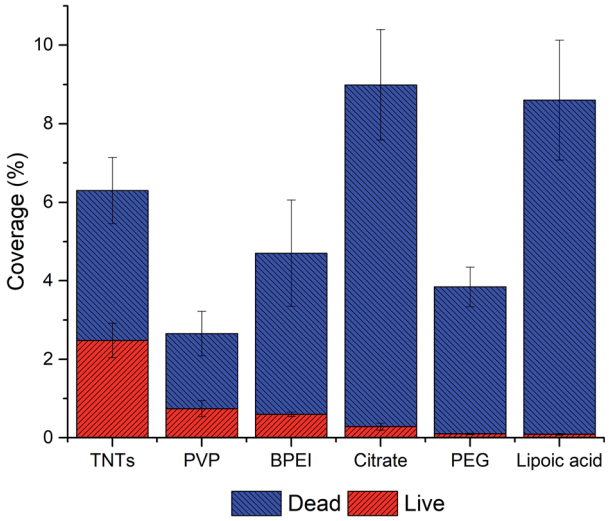

Fig. 6 The adhesion and live/dead assay of *E. coli* on AgNPs-TNTs surfaces. Data is expressed in % of total image area. All samples showed statistically significant difference ($p < 0.05$).

Adhesion and viability assay of G^- bacteria

The evaluation of the adhesion and viability of bacteria on AgNPs-TNTs surfaces, *E. coli* was chosen as a first representative model of Gram-negative bacteria. Some strains of *E. coli* are known for biofilm formation, which can be the source of persistent medical-device related infections.[47,48] SEM microphotograph (Fig. 5A) shows *E. coli* growing and colonizing control TNTs surface. Live/dead images and image analysis of *E. coli* after 24 hours' incubation shows the antibacterial activity of AgNPs-TNTs depending on the variability of nanoparticle functionalization layers (Fig. 5B and 6). The bacterial nucleic acid was stained with two fluorescence dyes, SYTO9 and propidium iodide, respectively. Green stain SYTO9 is cell membrane permeant, thus is stains nucleic acids of viable cells. On the contrary, red stain propidium iodide is membrane impermeable, it is commonly used to detect dead cells in a population. However, when the DNA is exposed to both stains, propidium iodide shows higher affinity to intercalate DNA and it is able to replace SYTO9. Therefore, the red fluorescence signal is generally considered as dead cell and green signal as live cell.[49,50] The non-decorated TNTs surface (control) showed almost 40% of dead *E. coli* bacteria, whereas nanoparticle-coated TNTs exhibited enhanced antibacterial activity as it is shown in Fig. 6. The live/dead ratio obtained from the image analysis determined the enhanced antibacterial activity of the sample as follows: TNTs > PVP > BPEI > citrate > PEG > lipoic acid (Table 2). The antibacterial activity of TNTs as control is in a good agreement with previous studies suggesting the antibacterial properties of annealed unmodified TiO_2 nanotubes.[32,51,52]

Generally, Ag nanoparticles significantly enhanced the antibacterial properties of TNTs in term of the amount of dead *E. coli* bacteria. Especially, lipoic acid and citrate functionalized AgNPs-TNTs samples showed a very low value of live/dead ratio (Table 2). However, when considering the total coverage of the surface with *E. coli*, which corresponds with the adhesion of

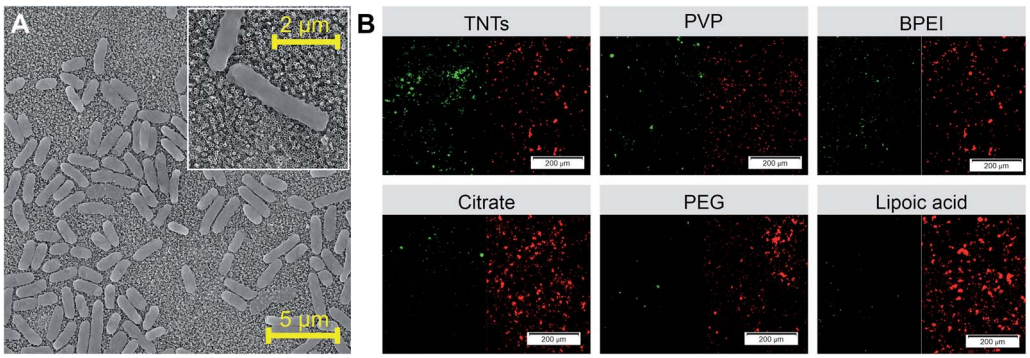

Fig. 5 SEM image of *E. coli* grown on control TNTs surface with bacteria detail showed in the insert (A). Live/dead fluorescence staining of *E. coli* performed on differently functionalized Ag-NPs decorating TNTs nanotubes ((B) red color represents dead cells and green color represents live cells). Abbreviations: PVP (polyvinylpyrrolidone), BPEI (branched polyethyleneimine), PEG (polyethylene glycol).

Table 2 The live/dead ratio of G^- and G^+ bacteria on TiO_2 nanotubes decorated with differently functionalized Ag-NPs after 24 hour incubation

	Live/dead ratio		
	E. coli	*P. aeruginosa*	*S. aureus*
TNTs	0.652 ± 0.012	1.161 ± 0.05	1.168 ± 0.003
PVP	0.381 ± 0.008	0.099 ± 0.011	0.926 ± 0.012
BPEI	0.151 ± 0.004	0.093 ± 0.001	1.021 ± 0.020
Citrate	0.033 ± 0.002	0.101 ± 0.013	2.457 ± 0.035
PEG	0.026 ± 0.001	0.009 ± 0.0002	0.447 ± 0.011
Lipoic acid	0.010 ± 0.001	0.019 ± 0.001	0.621 ± 0.008

bacteria, "lipoic acid" and "citrate" samples showed significantly higher surface coverages compared to other samples. Contrary, the PVP sample showed the lowest total surface coverage but exhibited good bacteria survival. It is generally considered that the electrostatic interaction between negatively charged bacteria membrane and positively charged nanoparticles increases the antibacterial efficiency.[58] For instance, since the lipoic acid, citrate, and PVP have a negative charge at physiological pH,[53–55] the repulsiveness between negatively charged NPs and bacterial cells is supposed to dominate. However, a significantly high surface coverage on citrate and lipoic acid functionalized AgNPs–TNTs surface compared to PVP was observed. Further, the pKa value of TiO_2 is between 5.3–6.2.[56] It means that under the physiological pH, the surface is negatively charged, and thus it should also behave repulsively to bacteria. Contrary, when combining negatively charged TNTs and positively charged BPEI functionalized NPs, the surface coverage is lower than citrate, and lipoic acid functionalized AgNPs-TNTs surface. Thus, we did not find any correlation in bacteria adhesion depending on the surface charge and charge of bacterial membrane. It leads us to the conclusion that instead of electrostatic interaction, the topography and the chemical character AgNPs-TNT surfaces must be the key factor not only in cell–surface interaction and adhesion but also in viability of bacteria on such surfaces. The nanoparticles enhanced the antibacterial properties of TNTs, and more importantly, the nanoparticle functionalization layers significantly contributed to the antibacterial effect of AgNPs-TNTs surface against *E. coli*.

Further, we tested all samples against Gram-negative *P. aeruginosa*, which is also known for the biofilm formation. It is the second most common Gram-negative bacteria causing orthopedic implant infection[57] and multidrug resistance.[58] Fig. 7A and B shows the SEM image of *P. aeruginosa* on the control TNTs surface and live/dead staining of bacteria on AgNPs decorated TNTs with different nanoparticle functionalization layers, respectively.

The data from image analyses of live/dead staining of *P.aeruginosa* (Fig. 8 and Table 2) showed a significant decrease in bacteria adhesion on NPs decorated TNTs compared to the control TNTs and also compared to the results obtained from *E. coli* experiment. Results can be attributed to several factors, including the charge repulsiveness, different composition of bacteria membrane, topography and chemistry of TiO_2

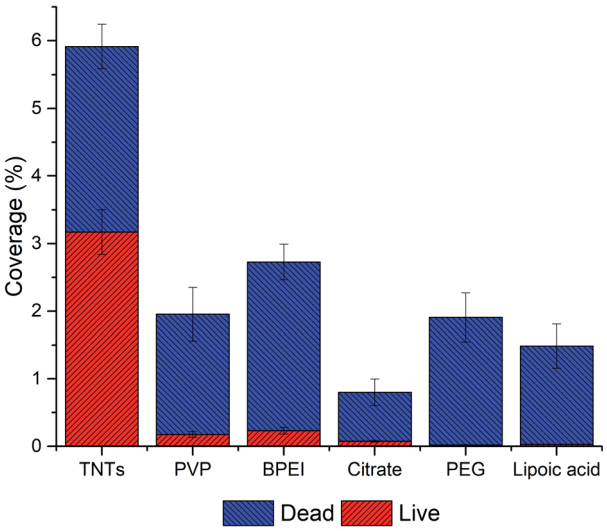

Fig. 8 Adhesion and live/dead assay of *P. aeruginosa* on AgNPs-TNTs surfaces. Data is expressed in percentage of total image area. All samples showed statistically significant difference ($p < 0.05$).

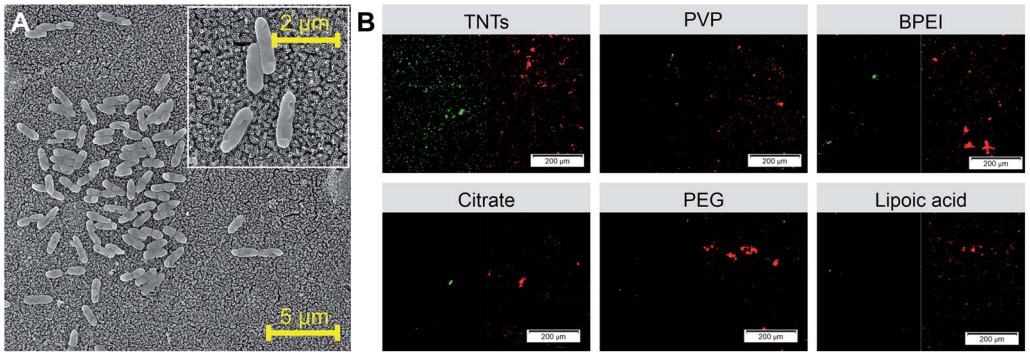

Fig. 7 SEM images of *P. aeruginosa* adhered on control TNTs sample and bacteria detail showed in the insert (A). Live/dead fluorescence images of *P. aeruginosa* adhered on differently functionalized Ag-NPs decorated on TNTs nanotubes ((B) red = dead cells; green = live cells). Abbreviations: PVP (polyvinylpyrrolidone), BPEI (branched polyethyleneimine), PEG (polyethylene glycol).

nanotubes and Ag nanoparticles.[59,60] These factors probably acted synergistically, as was demonstrated by our results. Additionally, the viability of *P.aeruginosa* on TNTs control was enhanced (~50%) compared to *E. coli* bacteria, and the lowest live/dead ratio has been found on PEG and lipoic acid samples which was also observed for *E. coli* bacteria. The similar live/dead ratio ~0.1 was calculated for PVP, BPEI, and citrate functionalized NPs.

Adhesion and viability assay of G^+ bacteria

S. aureus was chosen as a representative bacterial model for the evaluation of the adhesion and viability of Gram-positive bacteria on AgNPs-TNTs surfaces. In comparison to *E. coli* and *P. aeruginosa*, the primary source of hospital-acquired infections dwells in already infected people. *S. aureus* is biofilm-forming bacteria on bones, heart valves, or implanted materials.[61] Results obtained from live/dead assay suggested that *S. aureus* adhered well on nanoparticle decorated TNTs surfaces as well as on the control TNTs (Fig. 9 A and B). The bacterial coverage of surfaces with *S. aureus* (>32%) was several times higher than it was observed for Gram-negative bacteria (<9%). Moreover, the ratio of live/dead cells significantly increased, as shown in Fig. 10 and Table 2. For instance, the citrate functionalized NPs decorating TNTs showed a two-folded increase in live/dead ratio compared to the control TNTs.

The results demonstrated on *S. aureus* suggested that bacteria interact differently on AgNPs decorated TNTs surfaces as the increased adhesion and viability were observed compared to the G^- bacteria. *S. aureus* was also more resistant to the character of NPs functionalized layers. To get better antibacterial properties of AgNPs-TNTs surface against *S. aureus*, the increased number of nanoparticles on TNTs nanotubes should be performed and tested. On the other hand, it is also possible to think about absolutely different design of antibacterial surface for such resistant G^+ bacteria.

Colony counting assay of G^+ and G^- bacteria

Results from fluorescence staining showed the degree of bacterial adhesion after 24 hours and the living/dead cell ratio. Colony counting method performed in this work reflects the

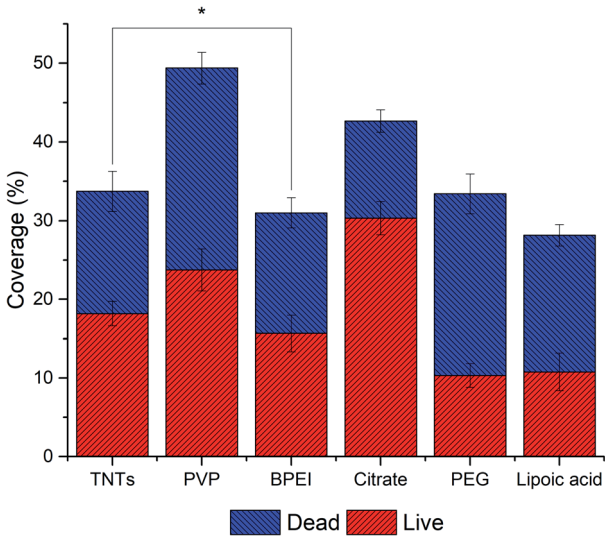

Fig. 10 Adhesion and live/dead assay of *S. aureus* on AgNPs-TNTs surfaces. Data is expressed in % of total image area. * indicates that there is no statistical significance ($p > 0.05$).

bacterial adhesion and viability after 4 hours' incubation of bacteria with AgNP-TNTs surfaces. Here, we performed colony counting assay for *E. coli* and *S. aureus* as representatives. Fig. 11A shows data obtained for *E. coli* bacteria, in which the adhesion and viability of bacteria decreased as follows: TNTs ≥ PVP ≥ BPEI > citrate > PEG > lipoic acid. The viability of bacteria corresponds with live/dead staining obtained for 24 hours, where the portion of living bacteria had the similar trend. Different results could be observed for bacterial adhesion at 4 hours and 24 hours. The shorter time of interaction between bacteria and surface followed the trend of bacteria viability. However, it was significantly changed when *E. coli* was exposed to the surface for 24 hours, in which the adhesion was increased on citrate and lipoic acid samples; although at the expense of more dead cells. The results obtained for *S. aureus* (Fig. 11B) after 4 hours' incubation of bacteria on the samples showed increased adhesion and viability as follows: TNTs ≥ PVP > BPEI ≥ PEG ≥ lipoic acid > citrate. Here we can see, that there is

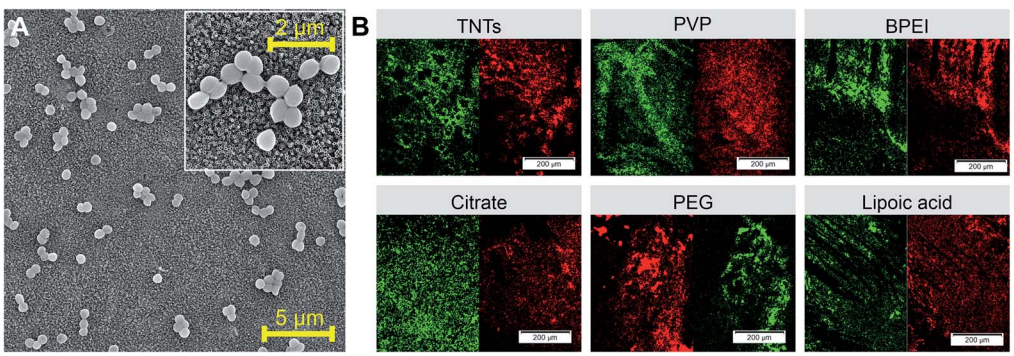

Fig. 9 SEM images of *S. aureus* adhered on the control TNTs sample with bacteria detail showed in the inset (A). Live/dead fluorescence staining of *S. aureus* performed on differently functionalized Ag-NPs decorated on TNTs nanotubes ((B) red color represents dead cells and green color represents live cells). Abbreviations: PVP (polyvinylpyrrolidone), BPEI (branched polyethyleneimine), PEG (polyethylene glycol).

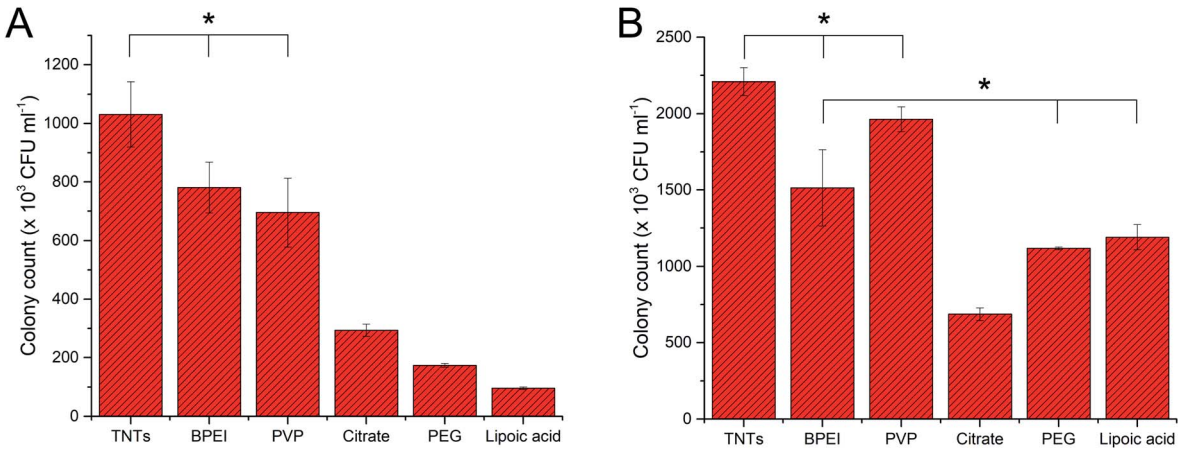

Fig. 11 The graphs of colony counting experiments expressed in colony forming units for *E. coli* (A) and *S. aureus* (B). Bacteria was exposed to surfaces for 4 hours, and the antibacterial effect was compared between individual samples. * indicates that there is no statistical significance.

a significant difference of results obtained for two incubation times. The explanation for this observation could be that bacteria sense, adhere and grow on different surfaces with different speed.

Conclusion

In this paper, the arrays of TiO_2 nanotubes were fabricated *via* single-step anodization of polished titanium foil. The nanotubes were decorated with silver nanoparticles stabilized with different functionalization layer such as polyvinylpyrrolidone, branched polyethyleneimine, citrate, polyethylene glycol, and lipoic acid. The antibacterial activity of Ag-decorated TiO_2 nanotubes was tested against three biofilm-forming bacteria, such as Gram-positive *S. aureus* and Gram-negative *E. coli* and *P. aeruginosa* using fluorescence microscopy-based live/dead assay and colony counting method. We showed that the stabilizing agent play important role in antibacterial properties of AgNPs as was confirmed by the synergistic effect of particular nanoparticles and TiO_2 nanotubes on adhesion and viability of G^- and G^+ bacteria. For future work, the antibacterial properties of TiO_2 nanotubes will be evaluated for different AgNPs concentrations and size and the cytocompatibility of such decorated nanotubes will also be in our interest.

Conflicts of interest

There are no conflicts to declare.

Acknowledgements

The authors wish to acknowledge the financial support of the GACR Project Number GA19-04270Y from the Czech Republic. This study was also supported by IGA MENDELU AFIGA2020-IP029 and ERDF "Multidisciplinary research to increase application potential of nanomaterials in agricultural practice" (No. CZ.02.1.01/0.0/0.0/16_025/0007314). We also thank to CEITEC Nano Research Infrastructure (LM2018110) and to Jan Prášek and Tomáš Lednický from CF Nano for AFM and XPS measurements.

References

1 R. J. Turner, Metal-based antimicrobial strategies, *J. Microb. Biotechnol.*, 2017, (10), 1062–1065.
2 A. Azam, *et al.*, Antimicrobial activity of metal oxide nanoparticles against Gram-positive and Gram-negative bacteria: a comparative study, *Int. J. Nanomed.*, 2012, (7), 6003.
3 A. Różańska, *et al.*, Antimicrobial properties of selected copper alloys on Staphylococcus Aureus and Escherichia Coli in different simulations of environmental conditions: with vs. without organic contamination, *Int. J. Environ. Res. Publ. Health*, 2017, (14), 813.
4 J. Hasan, *et al.*, Antibacterial surfaces: the quest for a new generation of biomaterials, *Trends Biotechnol.*, 2013, (31), 295–304.
5 J. A. Lemire, *et al.*, Antimicrobial activity of metals: mechanisms, molecular targets and applications, *Nat. Rev. Microbiol.*, 2013, (11), 371–384.
6 M. Mahlapuu, *et al.*, Antimicrobial Peptides: An Emerging Category of Therapeutic Agents, *Front. Cell. Infect. Microbiol.*, 2016, (6).
7 E. N. Gkana, *et al.*, Anti-adhesion and Anti-biofilm Potential of Organosilane Nanoparticles against Foodborne Pathogens, *Front. Microbiol.*, 2017, (8).
8 N. F. Kamaruzzaman, *et al.*, Antimicrobial polymers: The potential replacement of existing antibiotics?, *Int. J. Mol. Sci.*, 2019, (20), 2747.
9 V. Likodimos, Advanced Photocatalytic Materials, *Materials*, 2020, (13), 821.
10 A. Khezerlou, *et al.*, Nanoparticles and their antimicrobial properties against pathogens including bacteria, fungi, parasites and viruses, *Microb. Pathog.*, 2018, (123), 505526.
11 C. Buzea, *et al.*, Nanomaterials and nanoparticles: Sources and toxicity, *Biointerphases*, 2007, (2), MR17–MR71.

12 S. Wu, *et al.*, Antibacterial Au nanostructured surfaces, *Nanoscale*, 2016, (8), 26202625.
13 J. T. Seil and T. J. Webster, Antimicrobial applications of nanotechnology: methods and literature, *Int. J. Nanomed.*, 2012, (7), 2767.
14 G. Mohammadi, *et al.*, Development of azithromycin–PLGA nanoparticles: Physicochemical characterization and antibacterial effect against Salmonella typhi, *Colloids Surf. B Biointerfaces*, 2010, (80), 34–39.
15 Z. Fohlerova and A. Mozalev, Anodic formation and biomedical properties of hafnium-oxide nanofilms, *J. Mater. Chem. B*, 2019, (7), 2300–2310.
16 A. Tian, *et al.*, Nanoscale TiO2 nanotubes govern the biological behavior of human glioma and osteosarcoma cells, *Int. J. Nanomed.*, 2015, (10), 2423.
17 K. M. Kummer, *et al.*, Biological applications of anodized TiO2 nanostructures: a review from orthopedic to stent applications, *Nanosci. Nanotechnol. Lett.*, 2012, (4), 483–493.
18 X. Zhang, *et al.*, A functionalized Sm/Sr doped TiO2 nanotube array on titanium implant enables exceptional bone-implant integration and also self-antibacterial activity, *Ceram. Int.*, 2020, (46), 14796–14807.
19 Y. Cheng, *et al.*, Progress in TiO 2 nanotube coatings for biomedical applications: a review, *J. Mater. Chem. B*, 2018, (6), 1862–1886.
20 C. Mohan, *et al.*, In vitro hemocompatibility and vascular endothelial cell functionality on titania nanostructures under static and dynamic conditions for improved coronary stenting applications, *Acta Biomater.*, 2013, (9), 9568–9577.
21 Z. Fohlerova and A. Mozalev, Tuning the response of osteoblast-like cells to the porousalumina-assisted mixed-oxide nano-mound arrays, *J. Biomed. Mater. Res. B Appl. Biomater.*, 2018, (106), 1645–1654.
22 Q. Wang, *et al.*, TiO2 nanotube platforms for smart drug delivery: a review, *Int. J. Nanomed.*, 2016, (11), 4819.
23 H. Zhang, *et al.*, Improved antibacterial activity and biocompatibility on vancomycin-loaded TiO2 nanotubes: in vivo and in vitro studies, *Int. J. Nanomed.*, 2013, (8), 4379.
24 K. C. Popat, *et al.*, Decreased Staphylococcus epidermis adhesion and increased osteoblast functionality on antibiotic-loaded titania nanotubes, *Biomaterials*, 2007, (28), 4880–4888.
25 X. Zhang, *et al.*, Synergistic effects of lanthanum and strontium to enhance the osteogenic activity of TiO2 nanotube biological interface, *Ceram. Int.*, 2020, (46), 13969–13979.
26 J. Li, *et al.*, Plasmonic gold nanoparticles modified titania nanotubes for antibacterial application, *Appl. Phys. Lett.*, 2014, (104), 261110.
27 T. Yang, *et al.*, Cytocompatibility and antibacterial activity of titania nanotubes incorporated with gold nanoparticles, *Colloids Surf. B Biointerfaces*, 2016, (145), 597–606.
28 W. Liu, *et al.*, Synthesis of TiO 2 nanotubes with ZnO nanoparticles to achieve antibacterial properties and stem cell compatibility, *Nanoscale*, 2014, (6), 9050–9062.
29 O. Bilek, *et al.*, Enhanced antibacterial and anticancer properties of Se-NPs decorated TiO2 nanotube film, *PLoS One*, 2019, (14), e0214066.
30 W. Liu, *et al.*, Selenium nanoparticles incorporated into titania nanotubes inhibit bacterial growth and macrophage proliferation, *Nanoscale*, 2016, (8), 15783–15794.
31 M.-Y. Lan, *et al.*, Both enhanced biocompatibility and antibacterial activity in Ag-decorated TiO2 nanotubes, *PLoS One*, 2013, (8), e75364.
32 S. Mei, *et al.*, Antibacterial effects and biocompatibility of titanium surfaces with graded silver incorporation in titania nanotubes, *Biomaterials*, 2014, (35), 4255–4265.
33 Z. Guo, *et al.*, Fabrication of silver-incorporated TiO2 nanotubes and evaluation on its antibacterial activity, *Mater. Lett.*, 2014, (137), 464–467.
34 H. Li, *et al.*, Antibacterial activity of TiO2 nanotubes: influence of crystal phase, morphology and Ag deposition, *Appl. Surf. Sci.*, 2013, (284), 179–183.
35 U. F. Gunputh, *et al.*, Anodised TiO2 nanotubes as a scaffold for antibacterial silver nanoparticles on titanium implants, *Mater. Sci. Eng. C*, 2018, (91), 638644.
36 A. Roguska, *et al.*, Evaluation of the Antibacterial Activity of Ag-Loaded TiO2 Nanotubes, *Eur. J. Inorg. Chem.*, 2012, 5199–5206.
37 S. Yeniyol, *et al.*, Antibacterial activity of As-annealed TiO2 nanotubes doped with Ag nanoparticles against periodontal pathogens, *Bioinorgan. Chem. Appl.*, 2014, (2014), 829496.
38 N. Esfandiari, *et al.*, Size tuning of Ag-decorated TiO2 nanotube arrays for improved bactericidal capacity of orthopedic implants, *J. Biomed. Mater. Res.*, 2014, (102), 2625–2635.
39 A. Burkowska-but, *et al.*, Influence of stabilizers on the antimicrobial properties of silver nanoparticles introduced into natural water, *J. Environ. Sci.*, 2014, (26), 542–549.
40 D. van Phu, *et al.*, Study on antibacterial activity of silver nanoparticles synthesized by gamma irradiation method using different stabilizers, *Nanoscale Res. Lett.*, 2014, (9), 162.
41 L. O. Cinteza, *et al.*, Chitosan-stabilized Ag nanoparticles with superior biocompatibility and their synergistic antibacterial effect in mixtures with essential oils, *Nanomaterials*, 2018, (8), 826.
42 O. Bilek, *et al.*, Enhanced antibacterial and anticancer properties of Se-NPs decorated TiO2 nanotube film, *PLoS One*, 2019, (14), e0214066.
43 R. Vazquez-muñoz, *et al.*, Enhancement of antibiotics antimicrobial activity due to the silver nanoparticles impact on the cell membrane, *PLoS One*, 2019, (14), e0224904.
44 I. X. Yin, *et al.*, The Antibacterial Mechanism of Silver Nanoparticles and Its Application in Dentistry, *Int. J. Nanomed.*, 2020, (15), 2555–2562.
45 S. Prabhu and E. K. Poulose, Silver nanoparticles: mechanism of antimicrobial action, synthesis, medical applications, and toxicity effects, *Int. Nano Lett.*, 2012, (2), 32.

46 A. Borowik, *et al.*, The Impact of Surface Functionalization on the Biophysical Properties of Silver Nanoparticles, *Nanomaterials*, 2019, (9), 973.
47 T. Juhna, *et al.*, Detection of Escherichia coli in biofilms from pipe samples and coupons in drinking water distribution networks, *Appl. Environ. Microbiol.*, 2007, (73), 7456–7464.
48 Z. Khatoon, *et al.*, Bacterial biofilm formation on implantable devices and approaches to its treatment and prevention, *Heliyon*, 2018, (4), e01067.
49 S. M. Stocks, Mechanism and use of the commercially available viability stain, *BacLight*, 2004, (61A), 189–195.
50 M. Rosenberg, *et al.*, Propidium iodide staining underestimates viability of adherent bacterial cells, *Sci. Rep.*, 2019, (9), 6483.
51 B. Ercan, *et al.*, Diameter of titanium nanotubes influences anti-bacterial efficacy, *Nanotechnology*, 2011, (22), 295102.
52 A. Mazare, *et al.*, Corrosion, antibacterial activity and haemocompatibility of TiO2 nanotubes as a function of their annealing temperature, *Corros. Sci.*, 2016, (103), 215–222.
53 K. A. Huynh and K. L. Chen, Aggregation kinetics of citrate and polyvinylpyrrolidone coated silver nanoparticles in monovalent and divalent electrolyte solutions, *Environ. Sci. Technol.*, 2011, (45), 5564–5571.
54 Z. Qiao, *et al.*, Silver nanoparticles with pH induced surface charge switchable properties for antibacterial and antibiofilm applications, *J. Mater. Chem. B*, 2019, (7), 830–840.
55 K. Niska, *et al.*, Capping Agent-Dependent Toxicity and Antimicrobial Activity of Silver Nanoparticles: An In Vitro Study. Concerns about Potential Application in Dental Practice, *Int. J. Med. Sci.*, 2016, (13), 772–782.
56 X. van Doorslaer, *et al.*, UV-A and UV-C induced photolytic and photocatalytic degradation of aqueous ciprofloxacin and moxifloxacin: Reaction kinetics and role of adsorption, *Appl. Catal. B Environ.*, 2011, (101), 540–547.
57 L. Crémet, *et al.*, Orthopaedic-implant infections by Escherichia coli: Molecular and phenotypic analysis of the causative strains, *J. Infect.*, 2012, (64), 169–175.
58 N. M. Maurice, *et al.*, Pseudomonas aeruginosa Biofilms: Host Response and Clinical Implications in Lung Infections, *Am. J. Respir. Cell Mol. Biol.*, 2018, (58), 428–439.
59 P. R. Hunt, *et al.*, Bioactivity of nanosilver in Caenorhabditis elegans: Effects of size, coat, and shape, *Toxicol. Rep.*, 2014, (1), 923–944.
60 K. Vasilev, Nanoengineered antibacterial coatings and materials: A perspective, *Coatings*, 2019, **9**, 654.
61 J. L. Lister and A. R. Horswill, Staphylococcus aureus biofilms: recent developments in biofilm dispersal, *Front. Cell. Infect. Microbiol.*, 2014, (4), 178.

